

Comprehensive two-dimensional gas chromatography–time-of-flight mass spectrometry (GC × GC-TOF) for high resolution metabolomics: biomarker discovery on spleen tissue extracts of obese NZO compared to lean C57BL/6 mice

Werner Welthagen,^{a,b} Robert A. Shellie,^c and Joachim Spranger,^{d,e} Michael Ristow,^{d,e} Ralf Zimmermann,^{a,b,f} and Oliver Fiehn^g

^aInstitute of Ecological Chemistry, GSF-Research Centre, Oberschleißheim, D-85764, Germany

^bAnalytical Chemistry, University of Augsburg, Augsburg, D-86159, Germany

^cMax-Planck-Institute of Molecular Plant Physiology, 14424, Potsdam, Germany

^dGerman Institute of Human Nutrition, Potsdam-Rehbrücke, Germany

^eCharité University Medicine Berlin, Germany

^fBIfA – Bavarian Institute of Applied Environmental Research and Technology, Augsburg, D-86167, Germany

^gDavis Genome Center, University of California, Davis, CA, 95616-8816, USA

Received 25 August 2004; accepted 1 September 2004

Comprehensive two-dimensional gas chromatography–time-of-flight mass spectrometry (GC × GC-TOF) was applied for the analysis of complex metabolite profiles from mouse spleen. The resulting two-dimensional chromatograms proved that mass spectral quality and sensitivity were largely improved by the enhanced resolution and zone compression, which are features of GC × GC operation, when compared to classical one-dimensional GC-TOF methods. The improved peak capacity of GC × GC allowed for peaks to be detected that could previously not be separated in one-dimensional GC. A measure of the combined power of chromatographic and mass spectral deconvolution resolution is called “analytical purity”, with higher values indicating less pure peaks. GC × GC-TOF lead to the detection of 1200 compounds with purity better than 0.2, compared to 500 compounds with purity up to 2.5 in one-dimensional GC-TOF. The compounds identified include many of the compounds previously reported in NMR studies and other methods on mammalian tissues. Spleen samples of several obese NZO mice and lean C57BL/6 control strains were analyzed in order to demonstrate the applicability of GC × GC-TOF for biomarker identification.

KEY WORDS: Obesity, metabolomics; metabolic profiling; type 2 diabetes mellitus; nutrigenomics.

Introduction

A comprehensive and individual characterization of all the metabolites present in a given biological situation (metabolomics) is a challenging task for instrumental analysis. In the past 5 years, metabolomic strategies (Fiehn, 2002) have been developed mainly in the field of plant biology, with various applications being published (Weckwerth, 2004). These applications range from unraveling plant gene functions in physiological contexts (Weckwerth *et al.*, 2004a), to unbiased detection of unexpected metabolic responses under environmental stress conditions (Hirai *et al.*, 2004) or co-regulation of biochemical pathways that are commonly mapped far apart from each other (Fiehn, 2003). Protocols are adapted, tested and validated also for other organisms like bacteria (Wittmann *et al.*, 2004). Furthermore, alternative strategies have been applied to characterize global metabolic fingerprints in mammalian samples mainly by nuclear magnetic resonance spectroscopy (NMR) (Nicholson *et al.*, 1996). NMR metabolic fin-

gerprinting offers the advantage of truly quantitative measurements compared to mass spectrometry (MS), which relies on calibration or relative quantitations. However, NMR analyses lack the resolution and sensitivity required to individually quantify and identify the whole suite of metabolites present in typical biological samples. Typically, less than 30 signals can be referred to specific metabolites in NMR metabolic fingerprints (Keun *et al.*, 2002; Wang *et al.*, 2003).

The chemical diversity of metabolites can better be covered if at least two different physicochemical properties are exploited, like in gas chromatography–mass spectrometry (GC–MS: volatility and mass) (Fiehn *et al.*, 2000a, b) or high performance liquid chromatography–mass spectrometry (LC–MS: hydrophobicity and mass) (Tolstikov *et al.*, 2003). The combination of data from GC–MS and monolithic-LC–MS runs with the application of appropriate data deconvolution and extraction techniques enables the detection of some 1400 individual (and genuine) metabolites. The overlap between LC–MS and GC–MS with respect to the range of detectable compounds is limited due to the differences in

*To whom correspondence should be addressed.

E-mail: fiehn@mpimp-golm.mpg.de



73 separation and ionization mechanisms. An alternative
74 global approach that applied three different methods
75 based on capillary electrophoresis (CE) coupled to mass
76 spectrometry was elaborated, in which more than 1600
77 metabolites from *B. subtilis* cultures were detected (Sato
78 *et al.*, 2002). Although CE/MS is definitely stronger than
79 GC-MS, NMR or LC-MS with respect to phosphory-
80 lated or sulfated small molecules, it seems to be less
81 suitable for secondary metabolites and lipophilic com-
82 pounds. Difficulties with scaling up injection volumes
83 and capillary diameters further render CE/MS a less
84 suitable choice with respect to elucidating unknown
85 structures by fractionation and subsequent MSⁿ and
86 NMR analysis.

87 Researchers have recently tried to utilize the high
88 resolution of electrospray-ion cyclotron resonance-FT/
89 MS for annotating individual changes in metabolome
90 composition (Hirai *et al.*, 2004). Although direct infu-
91 sion-MS may be easily applied for sample classification
92 (Vaidyanathan *et al.*, 2001; Allen *et al.*, 2003; Scholz
93 *et al.*, 2004), relative quantitation of individual metab-
94 olites is problematic, due to severe physical limitations
95 such as ion suppression (Schmidt *et al.*, 2003) and
96 adduct formation. These fundamental constraints are
97 hardly solvable by current instrumentation, and lead to
98 major analytical errors in the comparison of samples
99 from different matrices, or in situations where largely
100 altered metabolite abundances occur, such as in com-
101 parisons of plant mutants or stress conditions.

102 A combination of GC-MS and LC-MS may be re-
103 garded as benchmark technique; however, with respect
104 to metabolome coverage, further improvements are
105 needed. Here we demonstrate for the first time in met-
106 abolomic analysis the use of a technique which signifi-
107 cantly enhances metabolite resolution: comprehensive
108 two-dimensional gas chromatography/time-of-flight
109 mass spectrometry (GC × GC-TOF). For proof of
110 concept we have selected an application in mammalian
111 biology: a comparison of two well-characterized mice
112 strains, namely obese NZO mice and C57BL/6 control
113 strains; and we exemplify how such profiles can be used
114 for biomarker detection. Spleen tissue was selected as
115 target for two reasons: (a) no report on metabolic pro-
116 files or NMR-based metabolic fingerprints from spleen
117 extracts has been published so far, and (b) obesity and
118 overfeeding have been demonstrated to negatively affect
119 immune response in humans as well as rodents (Lamas
120 *et al.*, 2004). We propose that metabolomics might help
121 in elucidating the underlying mechanisms.

Experimental

123 Mice were housed in standard barrier facilities
124 according to Federation of European Laboratory Animal
125 Science Associations (FELASA) regulations and were fed
126 standard chow (Altromin GmbH, Lage, Germany).
127 Spleen tissues were garnered from five female, non-fasted,

10 months old lean C57BL/6 control strain and four fe- 128
female, non-fasted, 10 months old obese NZO strain mice. 129
Five milligram fresh weight samples were extracted 130
at -15 °C with 1 ml of a mixture of degassed 131
H₂O:MeOH:CHCl₃ (2:5:2, v/v/v) and shaken for 5 min at 132
4 °C (Weckwerth *et al.*, 2004b). An aliquot of 500 μL was 133
concentrated to complete dryness. The dry residue was 134
dissolved in 20 μL of methoxamine hydrochloride 135
(40 mg/ml pyridine) and incubated at 30 °C for 90 min 136
with continuous shaking. Then 80 μL of *N*-methyl- 137
N-trimethylsilyltrifluoroacetamide (MSTFA) was added 138
to exchange acidic protons at 37 °C for 30 min. The 139
derivatized samples were stored at room temperature for 140
120 min before injection. A GC × GC system (Agilent 141
GC 6890, Agilent Technologies, USA; OPTIC III injector 142
ATAS, The Netherlands; cryogenic modulator and sec- 143
ondary oven: LECO Inc., USA) was coupled to a time-of- 144
flight mass spectrometer (Pegasus III, Leco Inc., USA). 145
The 4-jet cryogenic modulator uses two liquid nitrogen 146
cooled jets and two hot gas jets for efficient trapping and 147
re-desorption (gating) of the analytes (Ledford and 148
Billesbach, 2000; Kristenson *et al.*, 2003). Data acquisi- 149
tion and analysis was performed with a special software 150
package (ChromaTOF software, Version 2.00, LECO 151
Inc., USA). A two-column GC × GC column set was used 152
for all analyses, made up of a 30 m × 250 μm (0.25 μm 153
film thickness) dimethyl polysiloxane (Rtx-1MS, Restek 154
Corp., USA) first-dimension column, coupled to a 155
1.5 m × 100 μm (0.10 μm film thickness) 50% phenyl 156
polysilphenylene-siloxane (BPX-50, SGE, Australia) 157
second dimension column (press fit connection). Each 158
column was installed in an individual, independently 159
temperature programmable GC oven. The primary GC 160
oven (which housed the first-dimension column) was 161
temperature programmed from 50 °C (held for 8 min) to 162
310 °C at 5 °C/min. The secondary oven (second dimen- 163
sion column) was temperature programmed from 56 °C 164
(held for 10 min) to 300 °C at 5 °C/min. A modulation 165
period of 3.0 s was used. Constant flow rate was used 166
calculated from a linear flow rate of 20 cm/s at 25 °C. All 167
injections (1 μL) were performed in split mode (1:2) at a 168
constant injector temperature of 250 °C. The MS transfer 169
line temperature was kept at 280 °C, the ion-source tem- 170
perature was held constant at 250 °C, and the detector 171
voltage was -1.8 kV. Data were acquired at 100 spectra/s 172
(40–400 *m/z*). One-dimensional GC-TOF separation was 173
performed on a 30 m × 250 μm (0.25 μm film) dimethyl 174
polysiloxane (Rtx-1MS Restek) column under otherwise 175
same conditions as the two-dimensional separations 176
except a 10-fold higher sample injection due to lower 177
sensitivity in GC-TOF compared to GC × GC-TOF. 178

Results and discussion

180 Chromatograms of mouse spleen extracts (polar
181 fraction) exhibit a medium complexity when compared

182 to other specimen such as plant leaf samples. In figure 1,
 183 one- and two-dimensional separations of a spleen ex-
 184 tract are compared as total ion current (TIC) based
 185 chromatograms. In one-dimensional GC-TOF chroma-
 186 tograms (Figure 1a), 538 peaks were detected after
 187 deconvolution and artifact removal. There were many
 188 amino- and hydroxy acids among these detected peaks,
 189 but a limited number of (plant typical) carbohydrate
 190 derivatives were observed (supplemental table S1).
 191 Compared to early results from plant metabolite
 192 profiling by GC-quadrupole MS and manual chroma-
 193 togram inspection (Fiehn *et al.*, 2000a, b), the use of
 194 GC-TOF and mass spectral deconvolution increases the
 195 number of detectable peaks by a factor of three
 196 (Weckwerth *et al.*, 2004a). Mass spectral deconvolution
 197 is based upon slight differences in the time evolution of
 198 ions belonging specifically to different near co-eluting
 199 compounds. Not all of the detected peaks are immedi-
 200 ately visible in the TIC chromatogram because a high
 201 proportion of them are present as minor and/or poorly

202 resolved components. The apparent difference between
 203 the number of detectable peaks and the number of vis-
 204 ibly plotted peaks in TIC chromatograms (peak heights
 205 in figure 1a) highlights the importance of the data
 206 treatment by mass spectral deconvolution. The majority
 207 of low abundance peaks can only be observed by plot-
 208 ting a series of unique ion chromatograms, using the
 209 unique ions that the software automatically finds and
 210 reports for each detected peak. Despite these improve-
 211 ments, the deconvolution approach fails for fully co-
 212 eluting peaks or near co-elution of minor species with
 213 intense main compounds. This is specifically problem-
 214 atic when multiple chromatograms are to be compared:
 215 in such cases, subtle chromatographic shifts will cause
 216 overlapping of previously separated peaks, causing false
 217 negative peak detections and hence missing values.

218 GC \times GC-TOF enhances resolution and thus reduces
 219 the problem of co-eluting peaks (Marriott, 2002).
 220 Comprehensive two-dimensional gas chromatography
 221 (GC \times GC) was developed in the early 1990s (Liu and
 222 Philipps, 1991, Phillipps and Xu, 1995), and uses two
 223 serially coupled GC columns to separate compounds
 224 according to two different chromatographic selectivity
 225 parameters. The cryogenic modulation interface be-
 226 tween the two columns traps the eluted analytes from
 227 the first column for a short time and then releases them
 228 into the second column (Phillips and Beens, 1999;
 229 Marriott and Kinghorn, 2000). Following the conven-
 230 tions of the majority of published GC \times GC applica-
 231 tions (Marriott and Shellie, 2002), we have chosen to
 232 perform first-dimension separation on a relatively non-
 233 polar column, in which the separation approximates a
 234 boiling point separation, while the second separation
 235 was performed on a fast isothermal (moderately polar)
 236 50%-phenyl coated column for compound class separa-
 237 tion based on the components' relative polarity. As
 238 the second chromatographic separation lasts only some
 239 seconds (we here used a modulation period of 3 s), and
 240 since peak widths in GC \times GC are as narrow as 20 ms,
 241 a very fast responding detector is required. With spectral
 242 acquisition rates of up to 500 s⁻¹ a time-of-flight mass
 243 spectrometer is ideally suited for fast-GC (van Deursen
 244 *et al.*, 2000) and thus also for GC \times GC, specifically for
 245 separation of complex mixtures (Dallüge *et al.*, 2002a;
 246 Dallüge *et al.*, 2002b). The total run time from GC-TOF
 247 analysis of 65 min was pulsed into 1000 individual 3s
 248 modulation slices for GC \times GC-TOF with an acquisi-
 249 tion rate of 100 spectra/s, resulting in a total file size
 250 of 700 MB. Peak detection and deconvolution of
 251 GC \times GC-TOF chromatograms was performed as de-
 252 scribed above and was complemented by combination of
 253 thermally modulated peaks using the vendor's Chroma-
 254 TOF software. With a personal computer of 768 MB
 255 RAM and 2.0 GHz speed raw data processing took less
 256 than 30 min per sample.

257 Surprisingly, even for medium-complex samples like
 258 mouse spleen polar extracts, GC \times GC-TOF revealed a

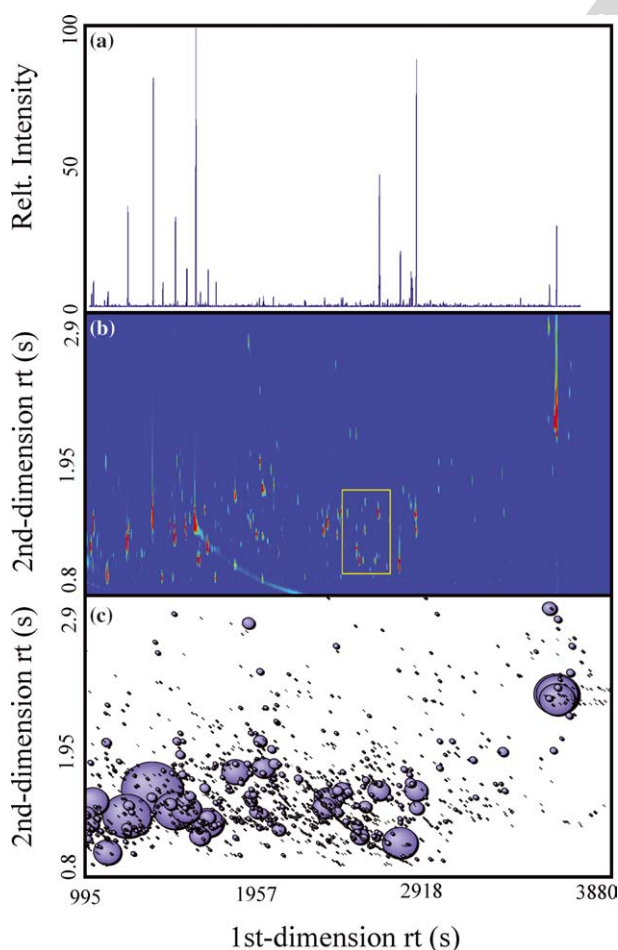


Figure 1. A comparison of a GC-TOF chromatogram analyzed independently (1a, top panel) with a GC \times GC-TOF two-dimensional chromatogram (1b, middle panel) of a NZO female mouse spleen extract. The lower panel (1c) is a bubble plot representation of the identified peaks in the GC \times GC chromatogram after the removal of known artifacts, with the bubble radius indicating the TIC intensity.

259 considerably higher number of separated peaks (Fig-
 260 ure 1b, peak intensity is given in color code from light
 261 blue to red). In excess of 1220 peaks were counted fol-
 262 lowing data treatment by deconvolution and removal of
 263 known artifacts such as polysiloxanes, phthalates or
 264 column bleed. Figure panel 1c gives a bubble plot
 265 representation of the same GC \times GC-TOF chromato-
 266 gram as in figure 1b, in which the size of the bubbles
 267 represents the TIC area of the respective chromato-
 268 graphic peaks. In comparison to figure 1b, this type of
 269 bubble plot presentation allows an improved overview
 270 of the peak distribution in the two-dimensional plane
 271 (Welthagen *et al.*, 2003; Shellie *et al.*, 2003). Table 1
 272 gives a comparison of GC-TOF to GC \times GC-TOF with
 273 respect to the resulting number and mass spectral
 274 quality of peaks. It becomes clear that overall, not only
 275 was the number of detectable metabolic peaks again
 276 increased by more than 2-fold, but also that analytical
 277 purity was greatly improved. Analytical purity refers to
 278 the combination of chromatographic resolving power
 279 and mass spectra deconvolution power. Therefore a
 280 compound may co-elute with other compounds yet still
 281 be pure if it's spectrum contains unique features relative
 282 to the co-eluting compounds. Obviously, it is more likely
 283 to achieve good purity if the chromatographic resolution
 284 is enhanced as in the case of GC \times GC-TOF. Purity
 285 approaches zero in the optimal case and can theoret-
 286 ically reach infinitum in problematic cases. We have
 287 found that spectra with purity < 1.0 are often the most
 288 trustworthy. Specifically for high throughput and un-
 289 supervised operation it is highly mandatory that only
 290 large and pure peaks are compiled in the list of target
 291 compounds. It is a clear advantage of GC \times GC-TOF
 292 analysis that there are about 7-fold more abundant and
 293 high quality peaks compared to one-dimensional GC-
 294 TOF, as defined by the threshold combination of S/N
 295 > 50 and purity < 1 . This finding was observed de-
 296 spite the total number of high abundance peaks being
 297 comparable and despite the roughly 10-fold lower
 298 sample injection into GC \times GC-TOF. This enhanced
 299 mass spectral quality is also reflected by the comparison
 300 of mean and median purity: most peaks in GC \times GC-
 301 TOF match the required quality thresholds. Corre-

spondingly, such peaks are more easily identifiable by
 matching to external spectral libraries and result in
 higher reliability in comparative quantifications between
 chromatograms.

A more detailed investigation of figure 1 leads to
 further insights to the advantages of GC \times GC appli-
 cations. For example, some problems with injection of
 silylated compounds are more clearly highlighted in
 GC \times GC than with one-dimensional GC-MS: ther-
 molabile compounds may partially decompose in the
 hot injector leading to characteristic sickle shaped ex-
 tended peak tailing (Beens *et al.*, 1998). An example of
 this is seen for tris-trimethylsilylated phosphoric acid
 (which partially also stems from decomposition of or-
 ganic phosphates), visibly tailing in figure 1b from
 about 1500–2100 s. This peak tail was therefore re-
 garded as artifact and removed from the data set (as
 seen in figure 1c) applying classification rules based on
 its mass spectrum. It should be noted that this unusual
 peak shape is not a result of GC \times GC, it is simply more
 noticeable in GC \times GC than in one-dimensional GC,
 where the low intensity peak tail would disappear below
 the chemical baseline (Shellie *et al.*, 2002). Despite the
 number of detectable peaks, only 126 peaks were posi-
 tively identified based on first-dimension retention index
 and mass spectral similarity when compared to a user
 library of 500 reference compounds (Figure 2 and sup-
 plemental table S1). Apart from classical biomedical
 targets such as glucose, fatty acids, amino acids and
 cholesterol, a range of other compounds were identified,
 among them dicarboxylic acids, aromatics and phos-
 phorylated sugars.

In figure 1b, a small area is marked (box) which is
 analyzed and discussed in more detail in the following

Table 1
 Comparison of number and quality of peaks by GC \times GC-TOF and
 GC-TOF from a mouse spleen extract after removal of known mea-
 surement artifacts

	GC-TOF	GC \times GC-TOF
# Compounds	538	1227
# With $S/N > 50$, Purity < 1	79	563
# With $S/N > 100$	202	342
Median purity	1.9	0.2
Mean purity	2.2	0.4
Median S/N	63	47
Mean S/N	411	310

Note: Threshold for peak detection was a signal/noise (S/N) ratio > 10 .

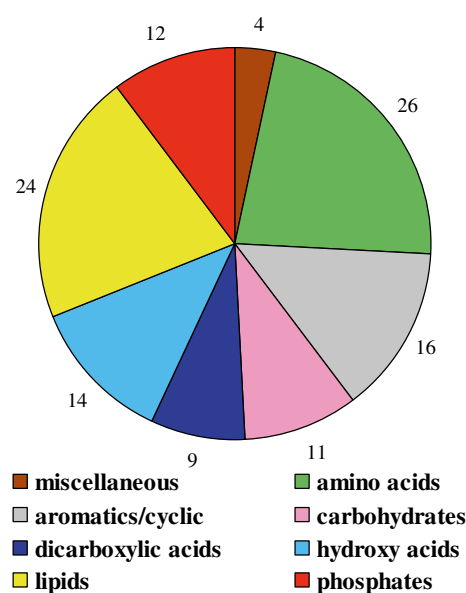


Figure 2. Compilation of identified peaks in GC-TOF based on
 first-dimension retention index and mass spectral similarity (see
 supplemental information table S1).

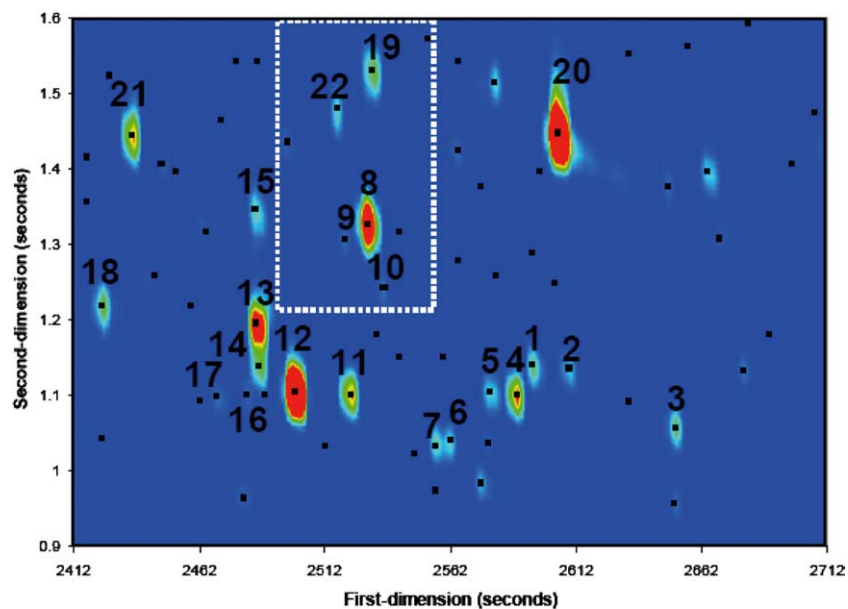


Figure 3. An extracted section from figure 1, showing the number of peaks detected (peak markers, black dots). Exemplary characterization of compounds is listed in table 2 (see supplemental information S2).

336 section. An enlarged representation of this area is shown
 337 in figure 3. The peak apex of each deconvoluted chro-
 338 matographic peak is represented by the peak markers
 339 (black dots). In total 69 separated peaks are found in
 340 this small section, from which 22 of the more abundant
 341 components are labeled by numbers and annotated in
 342 table 2. Furthermore their deconvoluted mass spectra
 343 are available as supplementary material S2. Most mass
 344 spectra show the characteristics of sugar alcohols such
 345 as inositol-like species, based on mass spectral similarity
 346 and retention indices of allo-inositol or methylinositol
 347 (ononitol). For a further identification, however,
 348 authentic references compounds are needed. Neverthe-
 349 less, the sheer complexity of detected sugar alcohol
 350 analogues might add potential hypotheses to the well-
 351 known involvement of inositol-phosphates in signaling
 352 cascades, which have been associated with diseases like
 353 diabetes and cancer (Cantley, 2002; Pendaries *et al.*,
 354 2003) both known to be caused and/or promoted by
 355 elevated body weight (Adami and Trichopoulos, 2003).
 356 Within the section marked by the indicated box in fig-
 357 ure 3, two peaks (#8 and #19) are present which com-
 358 pletely co-elute in the first-dimension and thus can be
 359 taken as an example to demonstrate the enhancement of
 360 resolving power gained by the GC \times GC approach. One
 361 of the two peaks (#8) is identified as ascorbate with a
 362 unique ion signal at 332 m/z , while the second peak
 363 (#19) indicates an unclassified and low abundant com-
 364 pound with a unique ion trace at 260 m/z . In figure 4 the
 365 corresponding section of the one-dimensional GC-TOF
 366 chromatogram is shown at the selected ion traces of 260
 367 and 332 m/z (left panel). Complete co-elution of these
 368 two compounds hampers the spectral quality of the
 369 more abundant compound (#8, ascorbate) and renders

the minor compound (#19) undetectable (false negative). 370
 In comparison, these two compounds can be nicely 371
 separated by GC \times GC-TOF (figure 4, right panel) with 372
 baseline separation in the second chromatographic 373
 dimension. This serves as an example of why (a) con- 374
 siderably more compounds are detected in GC \times GC- 375
 TOF than in one-dimensional GC-TOF, and equally 376
 important, why (b) the mean spectral purity in two- 377
 dimensional analysis was largely improved. One could 378
 argue that these peaks would have been separable in a 379
 one-dimensional GC-TOF run using a column of dif- 380
 ferent polarity. However, although this is certainly true 381
 for a specific peak pair, this would only be achievable at 382
 the price of creating new co-elutions among the 1200 383
 detectable compounds. With a lack of a universally 384
 applicable procedure for stationary phase selection, one 385
 may initiate a process of trial-and-error in the hope of 386
 identifying a specific stationary phase column that pro- 387
 duces a globally optimized separation. However this still 388
 might not resolve key biomarker compounds. Con- 389
 versely, GC \times GC has the capacity to resolve many 390
 more peaks in a single one-shot analysis than any one- 391
 dimensional GC separation (of equivalent time). The 392
 three main benefits of the GC \times GC-TOF approach are 393
 therefore (1) the maximum comprehensive separation 394
 obtainable within a single chromatographic run, (2) the 395
 increased average mass spectral purities and (3) the in- 396
 creased sensitivity obtained by the zone compression 397
 property of the cryogenic modulation (Lee *et al.*, 2001). 398
 This is specifically important in studies that go beyond 399
 manual interpretation of chromatograms, but focus at 400
 high-throughput and high-quality routine operation in 401
 metabolomics, specifically with respect to an enhanced 402
 quality of database entries in automated sample identi- 403

Table 2
Statistical comparison of the NZO and C57BL/6 samples based on the normalized TIC areas of the peaks #1–22 (see figure 2)

Characterization	#1 Sugar alcohol	#2 Sugar alcohol	#3 Alloinositol	#4 Sugar alcohol	#5 Sugar alcohol	#6 Sugar alcohol	#7 Sugar alcohol	#8 Ascorbate	#9 Hexa-decanol	#10 Aliphate	#11 Glucose 2
#1 C57BL/6	56,720	52,250	92,612	73,081	42,061	63,604	72,299	120,720	14,332	24,352	327,211
#2 C57BL/6	62,135	58,085	65,086	66,772	44,549	49,052	54,050	184,949	17,229	43,653	95,061
#3 C57BL/6	71,009	58,267	68,591	169,460	65,843	41,146	60,940	449,600	29,179	46,648	167,862
#4 C57BL/6	78,088	88,013	52,562	102,396	58,584	112,483	9851	358,179	45,786	42,319	77,751
#5 C57BL/6	56,944	48,898	76,960	99,842	30,035	109,734	16,133	285,096	19,837	14,967	203,468
#6 NZO	96,930	78,118	73,496	492,382	82,530	22,620	35,512	377,627	12,209	23,472	514,798
#7 NZO	30,731	48,500	58,140	176,200	28,115	16,238	27,539	217,621	3225	22,039	201,053
#8 NZO	28,149	18,394	60,806	144,819	30,190	9784	17,337	235,705	360,274	14,068	105,187
#9 NZO	67,572	58,657	69,998	319,683	57,940	47,486	7110	595,831	25,265	48,833	195,967
<i>t</i> -Test	0.31	0.25	0.25	0.05	0.46	0.01	0.09	0.25	0.23	0.24	0.23
Characterization	#12 Glucose 1	#13 1-Methyl- glucoside	#14 Hexose per-TMS	#15 Carbohydrate	#16 Fructose 1	#17 Fructose 2	#18 Carbohydrate	#19 Unknown	#20 Palmitic acid	#21 Dehydro- ascorbate	#22 Unknown
#1 C57BL/6	1,708,058	401,629	62,354	27,735	65,472	51,881	60,959	128,229	1,285,134	249,157	70,254
#2 C57BL/6	561,250	410,345	45,363	67,510	24,839	30,289	59,338	108,346	1,371,230	170,164	62,444
#3 C57BL/6	974,027	372,706	117,987	87,977	7626	28,465	111,313	138,522	1,418,236	200,697	51,634
#4 C57BL/6	453,153	260,279	61,865	61,209	70,256	81,543	82,691	143,997	1,581,389	134,817	59,684
#5 C57BL/6	1,148,108	378,136	61,777	75,590	27,198	32,014	1,11,015	168,731	1,483,671	286,296	98,586
#6 NZO	2,396,508	3,21,972	279,864	49,650	61,950	36,373	129,275	91,555	1,374,199	1,374,199	36,545
#7 NZO	1,123,571	200,498	114,618	50,604	55,310	27,644	81,006	48205	1,710,279	84,244	53,513
#8 NZO	627,186	176,794	78,270	27,066	27,188	14,926	61,855	58,689	10,102,294	90,059	29,556
#9 NZO	1,215,808	342,825	187,833	63,270	35,696	31,863	79,870	78,558	1,452,628	1,47,252	37,160
<i>t</i> -Test	0.22	0.04	0.06	0.12	0.35	0.09	0.44	0.001	0.19	0.27	0.01

Note: Peaks are characterized by likely compound class based on mass spectral features if identity is unclear. Methoximated sugars result in double peaks (as for glucose and fructose) with incomplete derivatization resulting in peak #14.

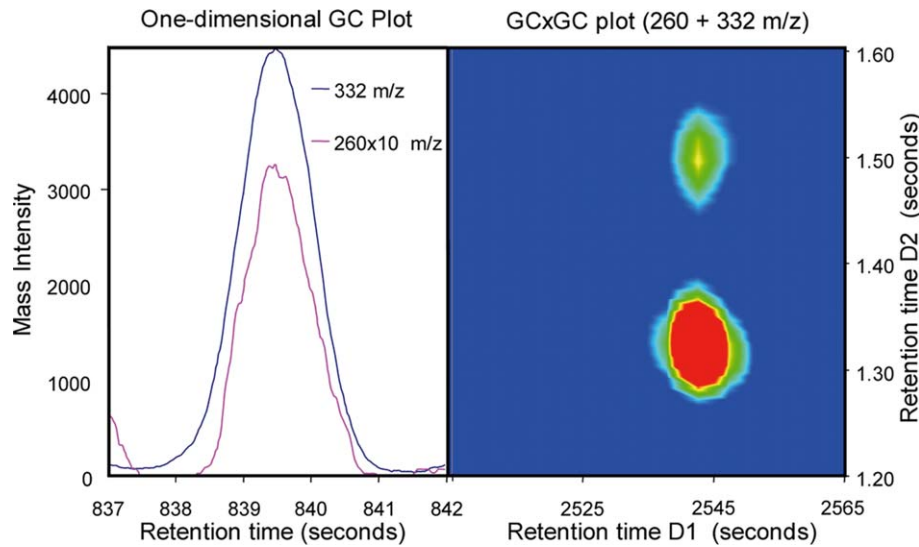


Figure 4. The co-elution of two peaks is indistinguishable in 1D GC-TOF (left panel), but clearly separated in GC \times GC-TOF (right panel). The more abundant peak is identified as ascorbate with a unique ion signal at 332 m/z , whereas the unknown compound has a unique ion of 260 m/z . The intensity of ion m/z 260 is given with a 10-fold enlargement in the one-dimensional GC-TOF ion chromatogram.

404 fication routines. Apart from an in-depth method vali- 408
 405 dation for high-throughput operation with respect to 409
 406 ruggedness, accuracy and reproducibility of quantita- 410
 407 tion, it is foreseeable that long-term data storage and 411

handling may get problematic with respect to the large 408
 size of the raw data files. 409

To demonstrate the usefulness of GC \times GC-TOF for 410
 differential metabolomic biomarker identifications, four 411
 non-fasted female NZO obese mice (#6–9) were 412
 compared to five non-fasted female C57BL/6 controls 413
 (#1–5). Sections of the corresponding nine GC \times GC- 414
 chromatograms are depicted in figure 5 using the same 415
 retention selection as indicated in figure 1. On the one 416
 hand, the chromatograms demonstrate the method 417
 reproducibility (i.e. stability of the separation pattern). 418
 For larger series of runs, potential shifts in first-dimen- 419
 sion retention times can easily be corrected for by using 420
 retention index markers. For shifts in the second 421
 dimension, absolute peak shifts are regularly less than 422
 the total peak widths which therefore gives an estimate 423
 for peak finding windows in differential analyses of 424
 series of chromatograms. On the other hand, in figure 5 425
 the biological variability between the individual mice 426
 becomes visually clear by the relative intensity differ- 427
 ences among the metabolites of either the control strain 428
 samples (left panel) or the NZO mice spleen extracts 429
 (right panel). Such biological variability largely exceeds 430
 the analytical error measured by repeated injections of 431
 identical extracts (~ 5 –10% relative standard deviation). 432
 Although the individuals belong to isogenic lines held 433
 under controlled environmental conditions, such a bio- 434
 logical variability is the expected result of metabolic 435
 snapshots (Steuer *et al.*, 2003). Still, systematic differ- 436
 ences can be observed which could be considered as 437
 potential obesity biomarkers: apparently, two sugar 438
 alcohols (peaks #6 and #7, indicated by yellow circles, 439
 numbering according to figure 3) are relatively less 440
 abundant in NZO spleen tissues compared to C57BL/6 441
 samples. To demonstrate a way to find differences be- 442

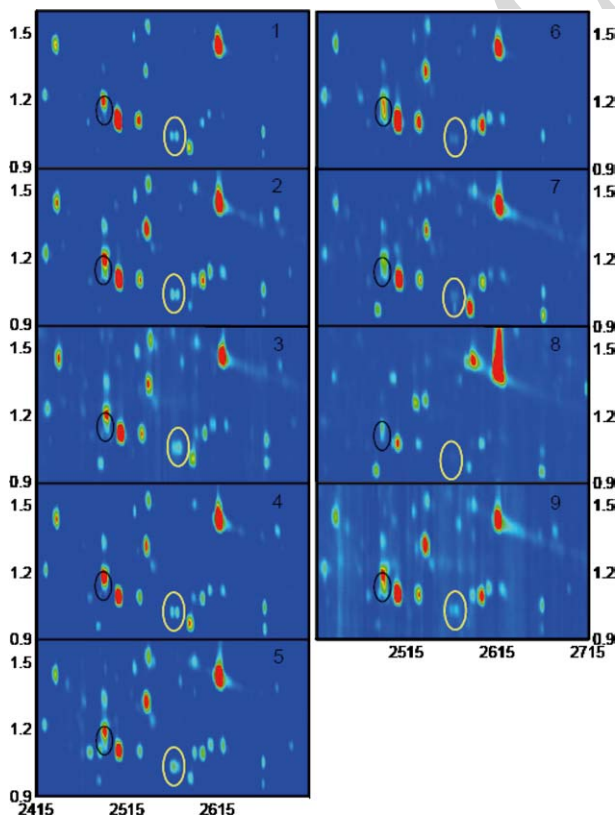


Figure 5. A direct comparison between the analyzed C57BL/6 female 404
 mouse spleen samples (left panel, samples 1–5) with the NZO female 405
 mouse samples (right panel, samples 6–9). The encircled compounds 406
 were used for exemplary statistical evaluation (table 2) of biomarker 407
 efficiency.

443 tween the two mice groups (NZO and C57BL/6), the
 444 peak areas of the individual peaks labeled in figure 3
 445 were normalized to the total area of all detectable peaks
 446 (after removing artifacts). Then, data were compared by
 447 Student's *t*-test (although it should be noted that the
 448 number of biological replicates *n* was too small to
 449 achieve actual statistical significance levels). Results are
 450 given in table 2 indicating that sugar alcohol #6 might
 451 indeed be different between the two groups whereas
 452 peak #7 had to be manually integrated to match the
 453 significance thresholds since it was below $S/N > 20$ in
 454 some of the obese NZO samples. Black circles in figure 5
 455 indicate 1-methylglycoside (peak #13) from figure 3:
 456 applying a *t*-test on the normalized peak areas,
 457 1-methylglycoside is also found as potentially different
 458 between the two mouse populations which was not
 459 visually apparent from the TIC chromatograms, as well
 460 as a further sugar alcohol (peak #4). Such initial
 461 hypotheses might then be tested by examining larger
 462 populations in order to gain statistical significance.
 463 Interestingly, the highest significance level and therefore
 464 the most likely obesity biomarker was found for peak
 465 #19: this was an unclassified, low abundant compound
 466 that was not separable from ascorbate in one-dimen-
 467 sional GC-TOF but only detectable by GC × GC-TOF.
 468 It is interesting to note that the most prominent meta-
 469 bolic changes in obese mice spleens were not related to
 470 classical analytical targets such as free fatty acids, glu-
 471 cose or cholesterol but to sugar alcohols and unidenti-
 472 fied compounds. This finding indicates the prospects as
 473 well as the problems of this technique for biomarker
 474 discovery: the technique is mature and can directly be
 475 applied for biomedical research; however, the diversity
 476 of the metabolome and the difficulties in *de novo* iden-
 477 tifications of GC-MS peaks (Fiehn *et al.*, 2000b) disable
 478 a direct and easy route to mapping differences in
 479 biochemical pathways.

Conclusion

481 It was demonstrated that extending GC-MS to the
 482 level of comprehensive GC × GC-TOF analysis is di-
 483 rectly applicable to differential metabolomic analysis of
 484 mammalian tissues. Apart from the increased number of
 485 safely detectable peaks, the most important feature is
 486 the enhanced spectral purity, which improves mass
 487 spectral deconvolution and similarity matches. This will
 488 certainly improve the data quality in biomedical data
 489 bases, if this technique is employed in larger research
 490 projects. In a proof-of-concept study on spleen extracts
 491 from lean versus obese mice strains, it was shown that
 492 data extraction and normalization tools are ready to be
 493 used for tentative biomarker detection. However, bio-
 494 logical variability demands a sufficient number of bio-
 495 logical replicates to be analyzed in order to suffice the
 496 required statistical power.

Acknowledgments

This work was financed through the GSF-research center, the Max-Planck-Society and the German ministry of education and research (BMBF), BioProfile Nutrigenomics Berlin/Brandenburg, BMBF project number 0313036B/C. We thank Anne Eckardt for quality control of extraction and GC-TOF standard operation procedures. Werner Welthagen thanks the Bayerische Forschungsförderung (BFS) for a scholarship. Michael Ristow is funded by the Deutsche Forschungsgemeinschaft and Fritz-Thyssen-Stiftung. Dr. R. Kluge and Dr. H.G. Joost gratefully provided NZO mice, and Dr. C. Thöne-Reinecke helped with animal handling.

References

- Adami, H.O. and Trichopoulos, D. (2003). Obesity and mortality from cancer. *N. Engl. J. Med.* **348**, 1623–1624. 512 513
- Allen, J., Davey, H.M. and Broadhurst, D. (2003). High throughput classification of yeast mutants for functional genomics using metabolic footprinting. *Nat. Biotechnol.* **21**, 692–696. 514 515 516
- Beens, J., Tijssen, R. and Blomberg, J. (1998). Comprehensive two-dimensional gas chromatography (GC × GC) as a diagnostic tool. *J. High Resolut. Chromatogr.* **21**, 63–64. 517 518 519
- Cantley, L.C. (2002). The phosphoinositide 3-kinase pathway. *Science*. **296**, 1655–1657. 520 521
- Dallüge, J., van Stee, L.L.P., Xu, X. *et al.* (2002). Unraveling the composition of very complex samples by comprehensive gas chromatography coupled to time-of-flight mass spectrometry, Cigarette smoke. *J. Chromatogr. A.* **974**, 169–184. 522 523 524 525
- Dallüge, J., Vreuls, R.J.J., Beens, J. and Brinkman, U.A.T. (2002). Optimization and characterization of comprehensive two-dimensional gas chromatography with time-of-flight mass spectrometric detection (GC × GC-TOFMS). *J. Sep. Sci.* **25**, 201–214. 526 527 528 529 530
- van Deursen, M.M., Beens, J., Janssen, H.-G., Leclercq, P.A. and Cramers, C.A. (2000). Evaluation of time of flight mass spectrometric detection for fast gas chromatography. *J. Chromatogr. A.* **878**, 205–213. 531 532 533 534
- Fiehn, O. (2002). Metabolomics – the link between genotype and phenotype. *Plant Mol. Biol.* **48**, 155–171. 535 536
- Fiehn, O. (2003). Metabolic networks of Cucurbita maxima phloem. *Phytochemistry*. **62**, 875–886. 537 538
- Fiehn, O., Kopka, J., Dörmann, P., Altmann, T., Trethewey, R.N. and Willmitzer, L. (2000). Metabolite profiling for plant functional genomics. *Nat. Biotechnol.* **18**, 1157–1161. 539 540 541
- Fiehn, O., Kopka, J., Trethewey, R.N. and Willmitzer, L. (2000). Identification of uncommon plant metabolites based on calculation of elemental compositions using gas chromatography and quadrupole mass spectrometry. *Anal. Chem.* **72**, 3573–3580. 542 543 544 545
- Hirai, M.Y., Yano, M., Goodenowe, D.B. (2004). Integration of transcriptomics and metabolomics for understanding of global responses to nutritional stresses in Arabidopsis thaliana. *Proc. Natl. Acad. Sci. USA.* **101**, 10205–10210. 546 547 548 549
- Keun, H.C., Beckonert, O., Griffin, J.L. (2002). Cryogenic probe ¹³C NMR spectroscopy of urine for metabolomic studies. *Anal. Chem.* **74**, 4588–4593. 550 551 552
- Kristenson, E.M., Kortjär, P., Danielsson, C., Kallio, M., Brandt, M. and Makela, J. (2003). Evaluation of modulators and electron-capture detectors for comprehensive two-dimensional GC of halogenated organic compounds. *J. Chromatogr. A.* **1019**, 65–77. 553 554 555 556 557

- 558 Lamas, O., Martínez, J.A. and Marti, A. (2004). Energy restriction
559 restores the impaired immune response in overweight (cafeteria)
560 rats. *J. Nutr. Biochem.* **15**, 418–425.
- 561 Ledford, E. and Billesbach, C. (2000). Jet-cooled thermal modulator
562 for comprehensive multidimensional gas chromatography.
563 *J. High Resol. Chromatogr.* **23**, 202–204.
- 564 Lee, A.L., Bartle, K.D. and Lewis, A.C. (2001). A model of peak
565 amplitude enhancement in orthogonal two-dimensional gas
566 chromatography. *Anal. Chem.* **73**, 1330–1335.
- 567 Liu, Z. and Phillips, J.B. (1991). Comprehensive two-dimensional gas
568 chromatography using an on-column thermal modulator inter-
569 face. *J. Chromatogr. Sci.* **29**, 227–231.
- 570 Marriott, P. and Kinghorn, R.M. (2000). New operational modes for
571 multidimensional and comprehensive gas chromatography by
572 using cryogenic modulation. *J. Chromatogr. A* **866**, 203–212.
- 573 Marriott, P. and Shellie, R. (2002). Principles and applications of
574 comprehensive two-dimensional gas chromatography. *Trends*
575 *Anal. Chem.* **21**, 573–583.
- 576 Marriott, P.J. (2002). Orthogonal GC–GC in Mondello, L., Lewis,
577 A.C. and Bartle, K.D. (Eds), *Multidimensional Chromatography*.
578 John Wiley & Sons, Chichester, England, pp. 77–108.
- 579 Nicholson, J.K., Foxall, P.J.D., Spraul, M., Farrant, R.D.
580 Lindon, J.C. (1996). 750 MHz ¹H and ¹H–¹³C NMR spectroscopy of human blood plasma. *Anal. Chem.* **67**, 793–811.
- 582 Pendaries, C., Tronchère, H., Plantavid, M. and Payrastre, B. (2003).
583 Phosphoinositide signaling disorders in human diseases. *FEBS*
584 *Lett.* **546**, 25–31.
- 585 Phillips, J.B. and Beens, J. (1999). Comprehensive two-dimensional gas
586 chromatography: a hyphenated method with strong coupling
587 between two dimensions. *J. Chromatogr. A* **856**, 331–347.
- 588 Phillips, J.B. and Xu, J. (1995). Comprehensive multi-dimensional gas
589 chromatography. *J. Chromatogr. A* **703**, 327–334.
- 590 Schmidt, A., Karas, M. and Dülcks, T. (2003). Effect of different
591 solution flow rates on analyte ion signals in nano-ESI MS, or:
592 when does ESI turn into nano-ESI. *J. Am. Soc. Mass Spectrom.*
593 **14**, 492–500.
- 594 Scholz, M., Gatzek, S., Sterling, A., Fiehn, O. and Selbig, J. (in press).
595 Metabolite fingerprinting: detecting biological features by
596 independent component analysis. *Bioinformatics*.
- 597 Shellie, R., Mondello, L., Marriott, P. and Dugo, G. (2002). Charac-
598 terisation of lavender essential oils by using gas chromatography–mass spectrometry with correlation of linear retention
599 indices and comparison with comprehensive two-dimensional
600 gas chromatography. *J. Chromatogr. A* **970**, 225–234.
- Shellie, R.A., Marriott, P.J. and Huie, C.W. (2003). Comprehensive
602 two dimensional gas chromatography (GC × GC) and GC
603 × GC-quadrupole MS analysis of Asian and American ginseng.
604 *J. Sep. Sci.* **26**, 1185–1192.
- Soga, T., Ohashi, Y., Ueno, Y., Naraoka, H., Tomita, M.
606 Nishioka, T. (2003). Quantitative metabolome analysis using
607 capillary electrophoresis mass spectrometry. *J. Proteome Res.* **2**,
608 488–94.
- Steuer, R., Kurth, J., Fiehn, O. and Weckwerth, W. (2003). Observing
610 and interpreting correlations in metabolic networks. *Bio*
611 *informatics*. **19**, 1019–1026.
- Tolstikov, V.V., Lommen, A., Nakanishi, K., Tanaka, N. and
613 Fiehn, O. (2003). Monolithic silica-based capillary reversed-
614 phase liquid chromatography/electrospray mass spectrometry
615 for plant metabolomics. *Anal. Chem.* **75**, 6737–6740.
- Vaidyanathan, S., Rowland, J.J., Kell, D.B. and Goodacre, R. (2001).
617 Discrimination of aerobic endospore-forming bacteria via elec-
618 trospray-ionization mass spectrometry of whole cell suspensions.
619 *Anal. Chem.* **73**, 4134–4144.
- Wang, Y., Bollard, M.E., Keun, H. (2003). Spectral editing and
621 pattern recognition methods applied to high-resolution magic-
622 angle spinning 1H nuclear magnetic resonance spectroscopy of
623 liver tissues. *Anal. Biochem.* **323**, 23–26.
- Weckwerth, W. (2004). Metabolomics in systems biology. *Annu. Rev.*
625 *Plant Biol.* **54**, 669–689.
- Weckwerth, W., Ehlers, M.L., Wenzel, K. and Fiehn, O. (2004).
627 Metabolic networks unravel the effects of silent plant pheno-
628 types. *Proc. Natl. Acad. Sci. USA* **101**, 7809–7814.
- Weckwerth, W., Wenzel, K. and Fiehn, O. (2004). Process for the
630 integrated extraction, identification and quantification of
631 metabolites, proteins and RNA to reveal their co-regulation in
632 biochemical networks. *Proteomics*. **4**, 78–83.
- Welthagen, W., Schnelle-Kreis, J. and Zimmermann, R. (2003). Search
634 criteria and rules for comprehensive two-dimensional gas
635 chromatography-time-of-flight mass spectrometry analysis of
636 airborne particulate matter. *J. Chromatogr. A* **1019**, 233–249.
- Wittmann, C., Kromer, J.O., Kiefer, P., Binz, T. and Heinzle, E.
638 (2004). Impact of the cold shock phenomenon on quantification
639 of intracellular metabolites in bacteria. *Anal. Biochem.* **327**,
640 135–139.
- 642